Algorithm Theoretical Basis Document
Chlorophyll Fluorescence (MODIS Product Number 20)

Mark R. Abbott

Ricardo M. Letelier

College of Oceanic and Atmospheric Sciences

Oregon State University

1.0 Introduction

The chlorophyll fluorescence product group (MODIS Product 20) includes several parameters. Two of these parameters will be described in the document: fluorescence line height (parameter 2575) and chlorophyll fluorescence efficiency (parameter 3211). In this document, we will discuss Version 2.0 of the algorithms associated with these two parameters. Chlorophyll fluorescence line curvature (parameter 2573) will be produced by Hoge and will be described in a separate ATBD.

In response to the first review, we have also accelerated plans to develop a primary productivity research product that will utilize the fluorescence data. We emphasize that this is a research product only and will not be part of the DAAC standard product suite. However, in the interest of completeness, we include a preliminary overview of this product in the ATBD. It will be produced in our Science Compute Facility (SCF) and will be available to any interested user.

The fluorescence line height algorithm is a relative measure of the amount of radiance leaving the sea surface, which is presumably a result of chlorophyll fluorescence. By constructing a baseline using bands on either side of the fluorescence band, we can estimate the deviation from the amount of radiance expected for pure water that results from chlorophyll fluorescence. This increase in radiance (centered at 683 nm for chlorophyll) has been noted for decades in measurements of the light field in the ocean. This signal is generally weak, even in regions of high chlorophyll concentrations. To measure fluorescence, the signal to noise ratio (SNR) was increased for the fluorescence band and the adjacent "baseline" bands at 665.1 nm (band 13) and 746.3 nm (band 15). The fluorescence measurement itself is made at 676.7 nm (band 14) as a compromise between measuring the fluorescence peak (683 nm) and the presence of an oxygen absorption band at 687 nm.

The chlorophyll fluorescence efficiency algorithm is also straightforward. ARP (number of photons absorbed by phytoplankton) will be calculated as part of MOD22 by K. Carder. This product will be converted into radiance units. Fluorescence line height will be normalized by this modified ARP product. The resulting ratio will provide an estimate of the efficiency of the conversion of absorbed solar radiation into fluorescence by phytoplankton.

This document will describe fluorescence and its relationship to photosynthesis by phytoplankton. We will cover the main points of fluorescence physiology, in particular its relationship to photoadaptation. The fluorescence algorithm will be described, as well as how information on fluorescence will be used in oceanographic research. Although fluorescence has been used for decades to estimate phytoplankton chlorophyll concentrations, our eventual focus will be on its use in estimating primary productivity. Other ATBD's of interest include upwelling radiance by H. Gordon (MOD18), absorbed photons by phytoplankton by K. Carder (MOD22), and primary productivity by W. Esaias (MOD27).

2.0 Overview and Background

Fluorescence by the light-harvesting pigments of phytoplankton is one of the main pathways for the deactivation of photosystem II (responsible for over 95% of chlorophyll fluorescence). This portion of the

photosynthetic cycle (PS II) is responsible for the splitting of water molecules and the formation of oxygen. NADP reduction takes place in photosystem I (PS I), and this photosystem is only weakly fluorescent. Together, PS I and PS II are known as the "light" reactions as they require light energy to proceed. The amount of fluorescence is a complicated function of light capture by chlorophyll and the rate of electron flow between PS II and PS I. Thus much attention has been focused on the use of fluorescence to estimate chlorophyll concentrations and primary productivity.

In the following sections, we will describe how such measurements are used, the historical basis for the algorithm, and how the algorithm is related to specific characteristics of the MODIS sensor.

2.1 Experimental Objective

Fluorescence line height (hereinafter referred to as FLH) will form the basis of chlorophyll fluorescence efficiency (hereinafter referred to as CFE) as well as for daily primary productivity (MOD27, parameter 2602) which will be a post-launch product. As fluorescence is an indicator both the amount of chlorophyll and the rate of photosynthesis, higher order products will be based on FLH.

Similar applications of fluorescence have been made in oceanographic and limnological studies using variants of the fluorometer. The basic fluorometric measurement was described by Holm-Hansen et al. (1965) and Lorenzen (1966); standard instruments were soon available, notably those made by Turner Associates, which was soon followed by Turner Designs. The basic measurement has been unchanged for nearly 30 years. A water sample is illuminated, usually by a blue light source, and the fluorescence emission is measured at 683 nm. Numerous improvements have been made in the electronics and optics of the sensors, resulting in a system that can work in turbid waters with either high sediment loading or high chlorophyll concentrations and can detect extremely low chlorophyll concentrations as well. An excellent summary of fluorescence can be found in Kiefer and Reynolds (1992).

The basic fluorometer has seen a wide range of modifications over the last decade. Spectrofluorometers (with varying excitation and emission wavelengths) have been used to study pigments other than chlorophyll *a*. Low-power fluorometers have been deployed on moorings and drifters. Light sources ranging from strobes to lasers have also been employed.

The primary use of fluorescence has been the estimation of chlorophyll concentration. With the development of flow-through sampling systems, it became possible to measure small-scale horizontal and vertical patchiness of phytoplankton abundance. Although data collection was fairly straightforward, the estimation of chlorophyll via fluorescence remained controversial. Most fluorescence studies collect occasional calibration samples where the pigment would be extracted from the phytoplankton, and chlorophyll would be measured using spectrophotometric methods. Between calibration samples, the ratio of chlorophyll to fluorescence was assumed to be constant. However, the literature is filled with studies that document the numerous processes that can change this ratio on a wide range of time and space scales. These processes included species changes, nutrient concentrations, incident radiation, etc. In essence, these processes are related to the physiological state of the phytoplankton.

Several modifications to the basic fluorescence method have been employed in an attempt to quantify the physiological state of the phytoplankton. This is based on the recognition that fluorescence instantly responds to all of the competing photosynthetic processes. A brief description of the process will help clarify matters. Within the phytoplankton cell, light is absorbed by chlorophyll molecules within the thylakoid membrane. Excitation energy is delivered to the reaction centers (where absorbed light energy is used in the photochemical process) by the proximal and distal antenna systems. When the reaction centers are "open", excitation energy can be trapped by passing electrons through an intermediate phaeophytin (a pigment related to chlorophyll) to a quinone acceptor (Q_A) and then used to oxidize water (PS II). If Q_A is already reduced by a previous excitation, then the reaction center is said to be "closed." The probability that the excitation energy will be fluoresced increases significantly when the reaction center is closed. Thus the intensity of fluorescence will depend on how much light is absorbed, how efficiently it can be delivered to the reaction centers, and how fast the absorbed (excitation) energy can be passed through the photosynthetic system. One can view the entire process as "the controlled production and dissipation of an electrochemical gradient where oxidation of water provides a source of free electrons

and the initial driving energy is free energy released by the de-excitation of an excited pigment molecule" (Falkowski and Kiefer 1985).

This coupling between fluorescence and the rate of photosynthesis has intrigued researchers for many years. Samuelsson and Öquist (1977) suggested that the addition of a photosynthetic inhibitor (DCMU, a common herbicide) could be used to separate the effects of light absorption (as an indicator of chlorophyll concentration) from light utilization (photosynthesis). Although DCMU does block electron flow and thus stimulates fluorescence, there are numerous other processes that affect fluorescence yield. Again, DCMU-induced fluorescence, as with the basic fluorescence method, can be used as an indicator of various physiological processes within the cell, but the relationship is complex (Prézelin 1981).

Recent research has focused on the use of sun-stimulated fluorescence to estimate primary productivity (e.g., Chamberlin et al. 1990; Kiefer et al. 1989; Kiefer and Reynolds 1992; Stegmann et al. 1992; Abbott et al. 1995). Although there is a link between the rate of productivity and the rate of fluorescence, it is not straightforward. As noted by Falkowski and Kolber (1994), the quantum efficiency of photosynthesis varies inversely to the quantum efficiency of fluorescence. However, there is no simple predictor of photosynthetic quantum efficiency. Although Falkowski and Kolber (1994) suggest that sun-stimulated fluorescence may not work over the wide range of oceanic conditions, MODIS will only be able to make useful estimates of FLH in regions of moderate to high chlorophyll concentration. The development of a post-launch primary productivity algorithm based on FLH will focus on such research.

Early measurements of upwelled radiance in natural waters showed the presence of a distinct peak in the spectrum centered at 683 nm. As the height of this peak was related to the chlorophyll concentration, it was easily recognized as the fluorescence emission peak. Papers by Smith and Baker (1978; 1981) clearly show this phenomenon using high quality, narrow bandwidth radiance measurements. This effect has been studied by numerous researchers, including Gordon (1979), Topliss (1985), Topliss and Platt (1986), and Kishino et al. (1984).

Gower and co-workers were among the first researchers to suggest using this signal to estimate chlorophyll concentrations from aircraft and satellites. The principle was identical to the basic fluorometer; a light source (in this case, the sun) would stimulate the fluorescence reactions which would then be measured by a narrow band detector. Known as solar or sun-stimulated fluorescence and occasionally as passive or "natural" fluorescence, this technique would complement the more traditional method of ocean color remote sensing based on radiance ratios in the blue/green portion of the spectrum.

2.2 Historical Perspective

Neville and Gower (1977) described the first measurements of sun-stimulated fluorescence from aircraft. Gower's program continued through the late 1970's and early 1980's with more sophisticated sensors with more bands and narrower bandwidth, culminating with the FLI (Fluorescence Line Imager) instrument that was optimized for fluorescence measurements (Gower 1980; Gower and Borstad 1981; Gower and Borstad 1990). Similar sun-stimulated fluorescence measurements were made in Germany by Fischer and co-workers (Fischer and Kronfeld, 1990; Fischer and Schlüssel, 1990). The Airborne Oceanographic Lidar (AOL) operated by Hoge can also be run in passive mode.

The fluorescence peak at 683 nm is approximately Gaussian with a half-power bandwidth of 25 nm. The fluorescence intensity can vary by a factor of four based on laboratory studies and field measurements. This variation can be caused by changes in light intensity and nutrient stress (Kiefer 1973 a and b; Abbott et al. 1982), and the response can occur on time scales of a few seconds to several hours. Borstad et al. (1985) compiled FLH observations from several years and noted that the relationship between FLH and chlorophyll could vary by a factor of eight. They also noted that the relationship within a particular study region was quite good and that the variability occurred when comparing different studies. In general, FLH varies from 0.01 to 0.08 $W/m^2/sr/mm$ per mg Chl.

Radiance leaving the ocean undergoes several modifications before it reaches the sensor. There is the addition of reflected sun and sky light from the sea surface and scattered light from the intervening atmosphere. There is also absorption by gases in the atmosphere. Scattering effects are most

pronounced at shorter wavelengths, but the fluorescence line is located in region of the spectrum where there are several narrow absorption features. In particular, there is an oxygen absorption band at 687 and 760 nm as well as water vapor absorption band at 730 nm. This means the fluorescence band will no longer have a simple Gaussian shape.

There are several approaches to atmospheric correction. The first is to rely on reflectance (radiance:irradiance ratios) but this is not feasible for remote sensing. A second approach is to model the atmosphere as was done for the Coastal Zone Color Scanner. Third, we could use a linear or curved baseline through wavelengths that are less affected by atmospheric absorption and scattering. Finally, we could use a high spectral resolution sensor to avoid known absorption features, such as oxygen.

This algorithm will follow combination of the second, third, and fourth approaches, building on the work pioneered by Gower and co-workers. Gower used aircraft-based sensors to test various channels as a baseline to calculate FLH. Bandwidth and position were varied, and eventually they developed a simple linear model using three bands (Borstad et al. 1985). Although a linear baseline was used, Gower and Borstad (1987) suggested that a curved baseline might perform better. Gower used an algorithm that is quite similar to that proposed for MODIS using bands 13 (667 nm), 14 (678 nm), and 15 (748 nm). Although there was some dependence of FLH on altitude (implying that there were some atmospheric effects present in the measurements), it tended to be smaller than the natural variability of the fluorescence measurement itself.

Gower and co-workers (reported in Borstad et al. 1985) compared FLH with chlorophyll concentrations from several locations. First, recall that the fluorescence signal is reduced by oxygen and water vapor which erodes the long wavelength portion of the fluorescence peak. Second, we expect that there will be considerable variability in fluorescence yield which will further complicate the estimation of chlorophyll concentrations. Despite these challenges, the FLH method worked reasonably well, even in turbid coastal waters with a high inorganic sediment load. As suggested by Borstad et al. (1985), combining the FLH measurement with an independent estimate of chlorophyll concentration (using the blue/green ratio approach) will provide a powerful tool to assess the physiological state of the phytoplankton.

The input radiances will be the normalized water-leaving radiances from MOD18 by Gordon. These radiances are corrected for sun-sensor geometry as well as for atmospheric scattering and absorption. However, the latter part of this correction (atmospheric effects) will be relatively simple compared with the more complex Rayleigh and aerosol corrections used in the blue and blue-green portion of the spectrum. Rayleigh scattering will be small at these fluorescence baseline wavelengths, and aerosol scattering should not vary much across this wavelength span (H. Gordon, pers. comm.) Thus we will compute only a simple atmospheric correction as well as correct for changes in view angle and solar geometry.

2.3 Instrument Characteristics

The three primary bands for FLH are bands 13 (665.1 nm), 14 (676.7 nm), and 15 (746.3 nm). Because of the low signal associated with fluorescence, these bands must have a high SNR to detect variations in the signal. The bands must be relatively narrow to avoid absorption features in the atmosphere. They must also be stable in terms of both bandwidth and position because of the spectral proximity of these absorption features. The present design for MODIS meets these requirements.

3.0 Algorithm Description

In this section, we will describe the fundamentals of the FLH and CFE algorithms. The FLH algorithm will be based on the calibrated, normalized water-leaving radiances as described under MOD18 (see ATBD by H. Gordon). Thus the bulk of the calculations will occur within the procedures necessary to transform the sensor data into Level 2 radiances. CFE will rely on a combination of FLH and the number of photons absorbed by phytoplankton (ARP) which is described by K. Carder in the ATBD for MOD22.

4

3.1.1 Physics of the Problem

The initial step in the algorithm will be the estimation of calibrated, normalized water-leaving radiances for each of the MODIS ocean bands. This will include registration of the bands (so that each band corresponds to the same pixel on the Earth's surface), calibration, and atmospheric correction. The details of this processing may be found in the ATBD's developed by Gordon and Evans. Because of the low levels of water-leaving radiance in the fluorescence wavelengths and because the bulk of the atmospheric effects take place in the blue wavelengths, we do not anticipate that an especially sophisticated procedure for atmospheric correction will be required. However, one potential difficulty may be the effects of sea foam (Frouin et al. 1996). Gordon is investigating these processes as part of his research on atmospheric correction; as we shall show later, our analyses indicate that even a fairly crude estimate of atmospheric effects is sufficient. The dominant source of uncertainty in fluorescence-based measurements is in the physiological processes of the phytoplankton themselves (Letelier and Abbott, 1996).

Chlorophyll fluorescence will increase the amount of water-leaving radiance at 683 nm (Gordon 1979; Topliss 1985; Topliss and Platt 1986) than would be expected for chlorophyll-free water. The amount of this increase will depend on several factors including the specific absorption of chlorophyll, fluorescence quantum efficiency, the amount of incident sunlight, and various atmospheric effects. However, judicious choice of wavelengths should tend to minimize the effects of the atmosphere. Thus the main component of the algorithm is the estimation of the increased radiance caused by fluorescence. By defining a baseline underneath the expected fluorescence peak, one can estimate the relative contribution to the upwelled radiance field by chlorophyll fluorescence. This baseline will be linear, based on MODIS channels places on either side of the fluorescence peak. FLH will then simply be the intensity of upwelled radiance in MODIS band 14 (676.7 nm) above the baseline created from bands 13 (665.1 nm) and 15 (746.3 nm). The figure below shows a schematic of the FLH algorithm.
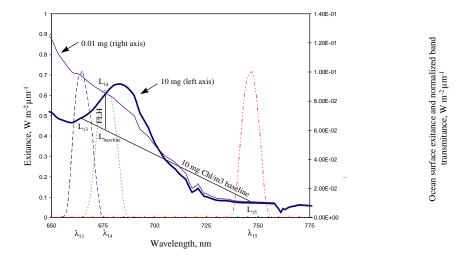

Figure 1. A schematic of the FLH algorithm, with dash/dot lines representing the normalized transmittance of MODIS bands 13, 14, and 15. The solid lines show the spectral distribution of upwelling radiance above the surface of the ocean for chlorophyll concentrations of 0.01 and 10 mg/m^3. The fluorescence per unit chlorophyll is assumed to be 0.05 W/m^2/μm/sr per mg chlorophyll. From Letelier and Abbott (1996).

Chlorophyll fluorescence efficiency refers to the conversion of incident sunlight into chlorophyll fluorescence. CFE requires an estimate of the amount of incoming solar radiation that is absorbed by phytoplankton in the near-surface waters since the fluorescence signal measured by MODIS will originate here. This estimate will be provided by MOD22 and is based on estimates of chlorophyll concentration, instantaneous photosynthetically available radiation, and the specific absorption of chlorophyll. Details can be found in the ATBD by Carder. The ARP product will be converted into radiance units as the original product will be expressed in terms of photons absorbed. Because the fluorescence peak can sometimes be below the baseline, we will add a constant radiance to all of the FLH values. This constant (0.05 W/m^2/μm/sr) corresponds to the minimum amount of fluorescence expected based on historical measurements. This modified FLH will then be normalized by the converted ARP to estimate CFE.
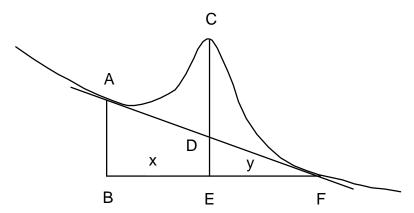
For both the FLH and CFE products, the input data sets will be level 2 data. For areas of chlorophyll greater than 1.5 mg/m^3, we will calculate FLH and CFE on a per pixel basis. For areas with chlorophyll less than 1.5 mg/m^3, we will examine 5 by 5 pixel regions to improve SNR in regions where the fluorescence signal will be small. First we will require that at least 16 of the 25 pixels be cloud-free in each superpixel. Second, we will average the appropriate input products (normalized water-leaving radiances, ARP) to decrease the noise level. We assume that noise will decrease as roughly $1/\sqrt{n}$, where n is the number of clear pixels.

3.1.2 Mathematical Description

The mathematics of both the FLH and the CFE algorithms are straightforward. After correcting for scan geometry, calibration, illumination, and the atmosphere, we take the normalized upwelled radiances as follows:

$$FLH = L_{14} - \left(\frac{L_{13} - L_{15}}{\lambda_{13} - \lambda_{15}} * (\lambda_{14} - \lambda_{13}) + L_{13} \right) \tag{1}$$

where the subscript refers to the MODIS band number. The formalism of (1) establishes a baseline between bands 13 and 15 and measure the peak height (band 14) above this baseline. A graphical representation of the algorithm is shown below:

In this representation, L_A is the short wavelength band, L_F is the long wavelength band, and L_C is the center or fluorescence wavelength. The distance between points B and E is denoted as *x* and the distance between point E and F is denoted as *y*. Using a simple like-triangles calculation, we may calculate FLH as:

$$FLH = CD = L_C - (L_F + DE) \tag{2}$$

This can be simplified as:

$$FLH = L_C - (L_F + ((L_A - L_F) * y / (x + y))) \tag{3}$$

In this case, we have simply rearranged (2) and expressed FLH as a linear function of the two baseline wavelengths and the fluorescence band.

CFE will be estimated by adding a constant radiance (FLH_{min}) to the FLH value and then normalizing by the radiance absorbed by phytoplankton in the upper ocean ($ARP_{radiance}$).

$$CFE = \frac{FLH + FLH_{min}}{ARP_{radiance}}$$ (4)

These algorithms have been embedded in the MODIS Oceans Team products processing system being developed at the University of Miami.

3.1.3 Performance and Uncertainty Estimates

A complete sensitivity analysis of the FLH algorithm is in press in *Remote Sensing of the Environment* (Letelier and Abbott, 1996). We present a summary of this paper here. As CFE is largely dependent on FLH, we expect that uncertainty in CFE will follow uncertainty in FLH.

There are three processes that will affect measurements of FLH. The first will be changes in the absorption and scattering properties of the atmosphere. Scattering will dominate at shorter wavelengths, but the presence of specific absorption features can be important in the fluorescence wavelengths. In particular, the oxygen absorption bands at 687 and 760 nm and the water vapor band at 730 nm will significantly influence the shape of the fluorescence peak such that it deviates from a pure Gaussian curve. By designing MODIS such that these absorption features are avoided, these problems are generally reduced. The second process involves the performance of the MODIS instrument itself. This is the only component that we can control (at least before launch). The final process is physiological change in the phytoplankton which will result in variability in FLH. As discussed earlier, this can be troublesome if we try to estimate chlorophyll concentrations from FLH as the amount of fluorescence per unit chlorophyll is not constant. The amount of fluorescence will vary as a function of the amount of light absorbed as well as the quantum efficiency of fluorescence. These quantities can vary according to the species and physiological state of the algae.

Specifications of the filter spectrum and signal to noise ratio (SNR) for each band are presented in Table 1. Based on Eq. 1 and assuming that noise is independent between bands, the SNR of the baseline may be calculated as

$$\frac{1}{SNR_{baseline}} = \frac{1}{SNR_{15}} + \left(\frac{1}{SNR_{13}} - \frac{1}{SNR_{15}} \right) * (\lambda_{15} - \lambda_{14}) / (\lambda_{15} - \lambda_{13})$$ (5)

The SNR of the FLH is calculated as:

$$\frac{1}{SNR_{FLH}} = \frac{1}{SNR_{14}} + \frac{1}{SNR_{baseline}}$$ (6)

Given the specifications of Table 1, the SNR of FLH is 752.

MODIS Band #	Center Wavelength	Tolerance		Bandwidth	Tolerance		Band SNR
		up	down		upper	lower	
	(nm)	(nm)	(nm)	(nm)	(nm)	(nm)	
13	665.1	1	2	10.3	4.2	6.1	1368
14	676.7	1	1	11.4	5.8	5.4	1683
15	746.3	2	2	10	5.1	5.3	1290

Table 1. Specifications for the fluorescence-related bands on MODIS (W. Barnes, pers. comm.)

A realistic range of upwelling radiance at the top of the atmosphere (TOA) for λ = 685 nm and a solar zenith angle of 50.7° is 8-20 W m^{-2} sr^{-1} μm^{-1} (Fischer and Schlüssel 1990). The lower end of this range corresponds to an atmospheric turbidity factor of 0.5 (visibility = 88 km), and the upper value corresponds to a turbidity factor of 10 (visibility = 6 km).   A similar value is obtained when the radiance spectrum at the TOA is calculated using a marine atmosphere model with a visibility of 50 km, a solar zenith angle of 60°, and the ocean spectrum without chlorophyll as input datasets for LOWTRAN 4.2 (Kneizys et al. 1988). The upwelling radiance at the TOA for λ = 685 nm obtained through this method is 8.65 W m^{-2} sr^{-1} μm^{-1}. However, given the characteristics of MODIS band 14, a more accurate estimate of the sensitivity is obtained by using the calculated TOA upwelling radiance at λ = 676.7 nm. In this case, the upwelling radiance at TOA calculated using LOWTRAN is 9.05 W m^{-2} sr^{-1} μm^{-1}. The TOA spectra are shown in the figure below.
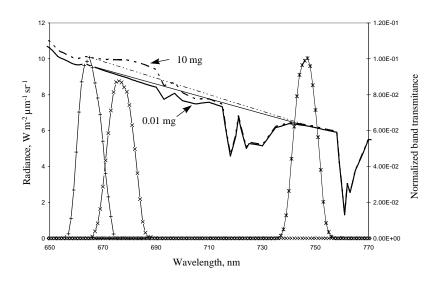

Figure 2. Baseline correction for the FLH algorithm for chlorophyll values of 0.01 and 10 mg/m^3 for spectra at the top of the atmosphere. From Letelier and Abbott (1996).

The minimum signal of detection (MSD) based on the SNR$_{FLH}$ and the TOA radiance at λ = 676.7 nm is :

$$MSD = \frac{Radiance_{TOA}}{SNR_{FLH}} = \frac{9.05 Wm^{-2}sr^{-1}\mu m^{-1}}{752} = 0.012 Wm^{-2}sr^{-1}\mu m^{-1} \qquad (7)$$

However, this MSD is calculated for an atmosphere with low turbidity. Under high turbidity, the MSD increases to 0.026 W m^{-2} sr^{-1} μm^{-1} and the sensitivity of the FLH algorithm decreases.

To convert MSD into chlorophyll, we must account for atmospheric attenuation, transmission through the air/sea interface, interference by suspended particulates, and variability in the fluorescence:chlorophyll ratio. For a typical mid-latitude oceanic atmosphere, the radiative transfer of the sea surface fluorescence signal measured at λ = 676.7 nm to the TOA is close to 80%. Increasing the ocean atmospheric aerosol content from a turbidity factor of 0.5 (visibility = 90 km) to a factor of 10 (visibility = 6 km) decreases the absolute atmospheric transfer of the fluorescence signal by less than 30%.   Variations in the atmospheric water vapor content also affect the recovery of the TOA fluorescence signal by less than 20%. These results are consistent with the results of the analyses performed by Fischer and Schlüssel (1990).

We believe that 30% is a conservative estimate of the loss of the fluorescence signal through the atmosphere. Hence, 0.017 W m^{-2} sr^{-1} μm^{-1} at λ = 676.7 nm is the minimum fluorescence signal at the ocean surface detectable at the TOA by the MODIS FLH algorithm.

Two processes contribute to a decrease of the upwelling radiance when the light crosses the sea-air interface. The principal process is refraction of light. The loss due to this process is approximately 45%. The second process is reflection. The loss in signal is small for angles of 0-40° to the vertical under calm conditions (2-6%) but can increase to 16-27% for the angles in the upper side of this range when the sea-surface becomes rough (Kirk 1994). By combining both processes, Austin (1980) proposes a correction factor of 0.544 to extrapolate the upwelling radiance at the sea surface to the upwelling radiance just below the surface.

If this correction factor is incorporated in the calculated minimum fluorescence signal measurable at the sea surface, the resulting minimum fluorescence signal in the upper water column required to be detectable by MODIS is 0.032 W m^{-2} sr^{-1} μm^{-1} at λ = 676.7 nm.

The conversion of this signal into chlorophyll values will depend on the fraction of energy absorbed by chlorophyll that is released in the form of fluorescence. This fraction is known as the chlorophyll fluorescence quantum yield (Φ_f):

$$FLH = \Phi_f * I_a \tag{8}$$

where I_a is the light flux absorbed by the photosystem. Because most chlorophyll fluorescence originates in PS II, I_a may be approximated by:

$$I_a = I_o * \sigma_{II} * n_{II} \tag{9}$$

where I_o in the mean incident irradiance, σ_{II} is the mean optical absorption of PS II, and n_{II} is the concentration of PS II, having a "typical" value of one unit per 500 chlorophyll *a* molecules (Kolber and Falkowski, 1993). However, under saturated light conditions I_a becomes independent from I_o. If we assume σ_{II} to be constant under light saturated conditions, the light flux absorbed per unit chlorophyll is nearly constant and the FLH per unit chlorophyll *a* is proportional to Φ_f as follows:

$$\frac{FLH}{Chl.a} = \Phi_f * \frac{I_a}{Chl.a} = cte.*\Phi_f \tag{10}$$

Published values of Φ_f vary between 0.0015 and 0.1 with a mean of 0.0035 (Fischer and Kronfeld 1990). However, based on field measurements, a range from 0.002 to 0.02 appears to cover most cases in marine environments (Gordon 1979). Fischer and Kronfeld (1990), assuming $\Phi_f = 0.003$, calculated a conversion factor of 0.05 W m^{-2} sr^{-1} μm^{-1} per mg chlorophyll at λ = 685 nm for light saturated photosynthetic conditions. A conversion factor of 0.057 W m^{-2} sr^{-1} μm^{-1} per mg chlorophyll at λ = 676.7 nm is found when reconstructing the chlorophyll fluorescence spectrum from the ocean surface spectra given by W. Barnes (pers. comm.). Using this conversion factor and the calculated detection limit of the fluorescence signal in the upper water column, based on the specified SNR, and the sea surface and atmosphere transmission, the limit of detection of changes in chlorophyll concentration is approximately 0.5 mg m^{-3} (Fig. 3). This limit of detection decreases to 1.3 mg m^{-3} under turbid atmospheric conditions.
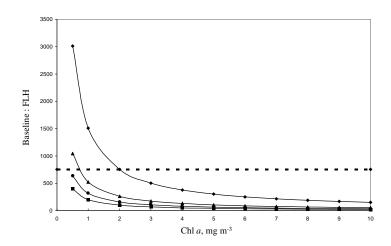
Figure 3. Detection limit of the FLH algorithm on a clear day (visibility = 90 km) as a function of the fluorescence to chlorophyll conversion factor ($\blacklozenge$ = 0.01, $\blacktriangle$ = 0.03, $\bullet$ = 0.05, $\blacksquare$ = 0.08 W m^{-2} μm^{-1} sr^{-1}). Values below the dashed line are detectable. From Letelier and Abbott (1996).

While atmospheric turbidity may strongly affect the limit of detection of the FLH algorithm by increasing the TOA radiance, the principal source of error in the interpretation of changes in the fluorescence signal arises from neglecting the role that algal physiology has in the production of fluorescence. The

fluorescence quantum yield (Φ_f) may vary an order of magnitude in marine environments as a result of changes in phytoplankton species composition, nutrient availability, temperature and light. The FLH signal per unit chlorophyll is proportional to Φ_f. Under light-saturated conditions, the detection limit of the FLH

algorithm cannot be defined in terms of chlorophyll unless Φ_f is known. The limit of detection under clear sky conditions may vary from less than 0.3 to greater than 2 mg m^{-3} when varying the fluorescence to chlorophyll conversion factor from 0.08 to 0.01W m^{-2} sr^{-1} μm^{-1} per mg chlorophyll (Fig. 3). Furthermore, observed spatial and temporal variations in the FLH signal do not necessarily reflect changes in chlorophyll concentration unless Φ_f is kept constant. Understanding the variability of the chlorophyll natural fluorescence due to changes in phytoplankton physiology is a critical step in the interpretation of changes observed in the FLH.

Other parameters that will affect the magnitude of the FLH signal are the size of particles and their effect on scattering, the concentration of suspended matter not containing chlorophyll, and the concentration of yellow substance (Gelbstoff). However, based on the results presented by Fischer and Kronfeld (1990), we have assumed that none of these parameters will modify the FLH by more than 30%. These effects are small compared with the potential variability introduced by changes in the atmosphere turbidity and chlorophyll fluorescence efficiency.

If noise is independent between pixels the SNR of individual bands increases fivefold when analyzing a 5 by 5 pixel signal. Hence, in areas of the ocean where surface water characteristics are homogeneous over scales larger than 5 by 5 pixels (nominally 25 km^2 at nadir), the limit of detection of chlorophyll concentrations for clear atmospheric conditions, assuming a conversion factor of 0.05 W m^{-2} sr^{-1} μm^{-1} per mg chlorophyll, decreases to 0.10 mg m^{-3}.

3.1.4 Algorithm Evolution

The first place for changes in the structure of the algorithm is in the area of atmospheric correction. However, the correction would essentially follow the same form as that for the other water-leaving radiances, as described by Gordon. To evaluate the performance a more sophisticated atmospheric correction, we would calculate FLH with both correction schemes and examine the data for systematic errors. Regions of persistent low humidity (such as at high latitudes) and high humidity (such as the tropics) will be candidate study areas as well as areas subject to rapid changes in air mass types, such as western boundary current regions. Time series of these areas will be examined for both systematic biases in the FLH estimates as well as for rapid shifts in FLH that might be indicative of changes in humidity. However, our error analysis (Letelier and Abbott 1996) suggests that even crude atmospheric corrections are a small part of the FLH error. The most important component of FLH error is the fluorescence quantum efficiency. Our primary focus over the next two years is to utilize variability in this efficiency to improve our estimates of primary productivity.

FLH is a measure of the absolute amount of energy released by phytoplankton in the form of fluorescence. This value is a function of the radiation absorbed by phytoplankton and the probability for a given absorbed photon to be re-emitted as fluorescence. This probability, known as the quantum yield of fluorescence (Φ_f) provides information with regard to the energy distribution in the photochemical apparatus (Krause and Weis 1991). To estimate the fluorescence quantum yield we plan on using the FLH product as well as the Absorbed Radiation by Phytoplankton (ARP) provided by Carder. Dividing FLH by ARP will allow us to estimate of the amount of energy absorbed by phytoplankton that is re-emitted as fluorescence, also termed chlorophyll fluorescence efficiency (CFE)

However, to derive photoautotrophic carbon fixation from APR and CFE we need to understand the relation between the fraction of energy used for carbon fixation (Φ_c) and the fraction released as fluorescence (Φ_f). Butler's tripartite model of the photosystem (Butler 1978) suggests that there is an inverse relationship between Φ_f and Φ_c However, this relationship is affected by environmental factors such as light saturation, nutrient limitation, and temperature.

To understand how nutrients and light affect the distribution of energy in the photosystem we are studying under controlled conditions the response of the photosystem to changes in light quality as well as to changes in nitrogen, phosphorus, and iron supply. Continuous cultures of different phytoplankton taxa are being grown in our laboratories, and we expect to have experimental results by the second trimester of 1997. The purchase of a Fast Repetition Rate (FRR) fluorometer will allow us to have continuous measurements of photosynthetic parameters such as the effective cross section of photosystem II and maximum change in quantum yield of fluorescence. Combining these measurements with measurements of solar induced (natural) fluorescence will help us to accurately interpret changes Φ_f and how they relate to changes in Φ_c. This is a critical piece of information required to develop a mechanistic model of primary production that uses phytoplankton natural fluorescence.

Much of this laboratory work is motivated by field observations of fluorescence made from quasi-Lagrangian drifting buoys that were equipped with spectroradiometers in the surface float. These sensors measure upwelled radiance at the SeaWiFS wavelengths as well as at 683 nm. Letelier et al. (1996) discuss results from a drifter deployment in the Southern Ocean. In this example, a drifter was deployed in the Drake Passage area in austral summer 1994-1995. A drogue was attached below the surface float so that the drifter would follow ocean currents at 15 m depth. We estimated chlorophyll using the radiance ratios developed by Clark (1981), analogous to the MODIS standard data product for chlorophyll. Fluorescence at 683 nm was corrected for backscatter using the 670 nm band; this is similar to the FLH approach for MODIS. Downwelling irradiance incident at the sea surface was measured using a single band (490 nm) irradiance sensor mounted on the top of the surface float. Together, the changes in amount of fluorescence per unit chlorophyll per unit sunlight are proportional to changes in Φ_f. Letelier et al. (1996) defined an apparent fluorescence quantum yield as the slope of the regression of fluorescence per unit chlorophyll and downwelling irradiance at 490 nm. This slope was based on 48-hour averages, thus eliminating the effects of diurnal photoadaptive processes.

This particular bio-optical drifter was trapped in a cyclonic eddy for over forty days. During this period, Letelier et al. (1996) calculated vertical velocity based on the conservation of potential vorticity and the measured horizontal velocities associated with the drifter displacement. Regular, short-term variations in the apparent fluorescence quantum yield were observed as well as in the relative depth of the eddy's upper layer. The correlation between layer thickness and fluorescence quantum yield are probably driven by changes in nutrient availability. Decreases in layer thickness correspond to upward vertical velocities. Rough estimates of the vertical velocity are on the order of 20-60 m/day. Given that iron is probably the limiting micronutrient in this region, we suggest that iron stress may be alleviated during these upwelling events, thus reducing the fluorescence quantum yield and increasing photosynthetic quantum yield. During downwelling, the situation is reversed (Fig. 4).
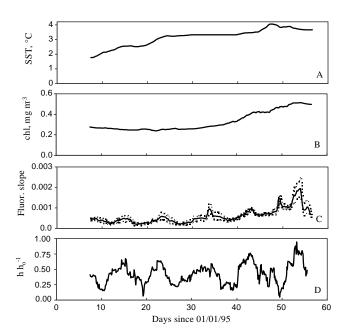

Figure 4. Temporal variability of (A) sea surface temperature, (B) chlorophyll concentration, (C) Apparent Φ_f, and (D) relative depth of the upper layer of the water column sampled by the drifter within the cyclonic eddy. Dotted lines in (C) show the 95% confidence interval. Note that the apparent fluorescence quantum yield (C) increases approximately one day after the relative thickness of the upper layer (D) begins to increase.

In regards to MODIS, it is interesting to note that the averaged estimates of fluorescence quantum yield seemed to fall into two categories, depending on the nutrient regime. As MODIS will observe the ocean only under conditions of full sunlight, we will not be able to conduct an analysis similar to the one used for the drifter data. However, if the fluorescence quantum yield falls only into a few, easily distinguishable categories, then we should be able to measure CFE with MODIS over a period of several days to estimate primary productivity. That is, the variability in CFE will give an indication of the photoadaptive state of the phytoplankton, information that in turn can be used to estimate the quantum yield of photosynthesis. We will be conducting both field and laboratory experiments (discussed earlier) to develop such a model.

The other potential area for evolution is the use of multiple data sources to estimate FLH. Besides AM-1 and PM-1, MERIS and GLI will also measure sun-stimulated fluorescence. Although the calculation of

FLH for each sensor will be essentially unchanged, blending of the data sets will require considerable research. Issues such as binning, which sensor to select in cases of multiple observations, cross-calibration, etc. will need to be addressed. The different crossing times for the various sensors that are capable of chlorophyll fluorescence measurements may allow us to refine our productivity models by examining daily variations in fluorescence quantum yield.

3.2 Practical Considerations

3.2.1 Programming and Procedural Considerations

The FLH algorithm is simple, as it is merely a manipulation of normalized, calibrated radiances from the Miami-developed ocean processing system. The bulk of the computation will take place in this system. After application of the FLH algorithm, the data will then be available for remapping into standard grids. The registration process will be part of the Miami system. CPU load should be relatively small; therefore the use of lookup tables (as opposed to direct calculation) will not be efficient. CFE is a simple combination of FLH and ARP. C code for both FLH and CFE has been delivered to Miami and integrated into the MODIS oceans processing.

A 5 by 5 array will be centered on each pixel. The algorithm will first check the corresponding chlorophyll from the Case 1 chlorophyll product calculated using Clark's algorithm (MOD19). If chlorophyll is less than 1.5 mg/m^3, then the radiances from the 5 by 5 bin will be averaged; this average will be used in the FLH and CFE calculations. The coefficient of variation will also be calculated. The 5 by 5 array will then be moved over one pixel, and the process will be repeated. At the end of the scan line, the array will be shifted up one line. Thus, the output product will consist of FLH and CFE calculated at every pixel, and the number of pixels used to calculate FLH may range from 1 to 25.

3.2.2 Calibration and Validation

Validation will rely on a three-part approach. The first approach will rely on systematic studies of large volumes of MODIS observations over several seasons to quantify spatial and temporal error patterns. The second component of our validation studies is an extension of this approach and relies on statistical comparisons of MODIS observations with similar measurements from MERIS and GLI. The third approach will be comprehensive in situ studies, conducted at a few representative sites in the world ocean that span a spectrum of oceanic and atmospheric conditions.

The basic FLH algorithm is a simple estimate of peak height. The more critical factor will be the assessment of instrument and atmospheric effects on the basic input data sets. The first stage in validation will be to compare the FLH results with other MODIS data products. For example, FLH should be similar to the patterns of chlorophyll; are there systematic differences? How does FLH compare with estimates of aerosol radiance? The next stage will be to compare FLH with geographic and geophysical properties. For example, are there systematic changes in FLH across a scan line, indicating a dependence on satellite look angle and hence path radiance? Does FLH change near the edges of clouds, where aerosol concentrations may be higher? Are there systematic seasonal changes? Other data sets such as wind velocities (from scatterometers) will be used in for validation. Our plan is to use large volumes of MODIS data products to seek out such systematic relationships.

The second approach to validation will be to compare MODIS estimates of FLH with other satellite-based estimates of FLH. Both MERIS and GLI will make measurements in the fluorescence region, although it is likely that the exact bands will differ slightly from MODIS. Thus such comparisons will not be based on exact comparison of FLH estimates from the same pixel location, but rather on general trends and patterns. For example, for regions that are simultaneously observed by MODIS and either MERIS or GLI will be analyzed for trends and biases. (In this case, "simultaneous" means within a few hours.) Such comparisons will allow us to examine estimates of FLH under different viewing conditions to characterize the effects of path radiance. These studies will be conducted in different geographic locations and in different seasons.

The final component of our validation plan relies on a set of focused in situ observations. The framework for field validation studies will be based on the framework developed for SIMBIOS. Our activities will build

on the foundation established for SIMBIOS in terms of protocols and data management. The basic water-leaving radiances for the FLH algorithm will be validated in a manner similar to the other ocean color bands as described by Gordon.

Because of the intense variability in the ocean on mesoscales along with lower frequency processes such as the El Niño/Southern Oscillation (ENSO) events, it is not possible to sample all of the critical conditions and regions adequately. Instead, intensive campaigns will be carried out a few sites that span a wide range of oceanographic and atmospheric conditions. To assess the effects of lower frequency variability, autonomous samplers will be deployed in a few locations for several years. These stations will be much less sophisticated than the bio-optical mooring developed for the SeaWiFS and MODIS by Clark. By keeping costs low, more sensors will be deployed as either fixed moorings or free-floating drifters in order to characterize temporal and spatial variability. The long-term goal of this approach is to develop a body of knowledge of the error fields of the data sets that can be used in data assimilation models.

Before the launch of EOS, we are planning extensive field measurements at two locations: the Joint Global Ocean Flux Study (JGOFS) site at the Hawaii Ocean Time-series (HOT) north of the island of Oahu and at the Polar Front as part of the JGOFS Southern Ocean study. The HOT effort is a new biogeochemical mooring that will be deployed at 157° 50'W, 23°N in conjunction with Station ALOHA which is located about 20 km away. The mooring (known as HALE ALOHA) will support meteorological, bio-optical, chemical, and physical measurements in the upper 300 m of the ocean. An automated water sampler will also be attached to the mooring. This site will complement the MOBY site which is located west of the island of Lanai and is focused more heavily on precise bio-optical measurements in support of SeaWiFS and MODIS calibration activities. Our contribution to the mooring will be two Satlantic irradiance sensors which will measure irradiance at the MODIS oceans wavelengths. The bio-optical measurements will be analyzed in conjunction with the more extensive suite of biological and chemical measurements to develop and validate productivity algorithms as well as assess processes that affect both FLH and CFE. We will also use our Fast Repetition Rate (FRR) fluorometer in this assessment. The second field site is part of the final U.S. JGOFS process study in the Southern Ocean known as Antarctic Environment Southern Ocean Process Study (AESOPS). We will deploy 12 bio-optical moorings in the Polar Front at 170°W, 65°S, relying primarily on funding from the National Science Foundation. This array will be established in October 1997 and remain in the water for five months. The moorings will consist of expendable current meters and Satlantic irradiance sensors. Bio-optical drifters will also be deployed during the 1997-1998 mooring experiment. (Three bio-optical drifters were deployed in the Polar Front in September 1996 using MODIS funding.) Ship-based observations will also be made to collect near-surface upwelled radiances, pigments, fluorescence, and primary productivity.

The approach begun in the pre-launch phase will continue after the launch of EOS AM-1 in 1998. The HALE ALOHA mooring work will continue at least until 2000. However, the Southern Ocean JGOFS program will have concluded, and we plan to continue Southern Ocean work in collaboration with Dr. John Parslow (CSIRO Australia). The study site will be at the Polar Front but farther west at 145° E. Measurements (moorings and drifters) similar to the JGOFS project will be conducted, but the density of sampling will be less. The focus of this experiment will be to estimate seasonal and interannual variability of the model parameters. We will participate in the MOCEAN joint experiment planned for the upwelling system off Northwest Africa in 1999. This experiment is focused more on the effects of atmospheric processes on the MODIS retrievals, especially in the presence of intense loading of dust from the Sahara. This region will provide a valuable comparison with the high latitude site at the Polar Front and the low latitude site off Hawaii where dust loading is much smaller. The last target area will be the productive waters off Oregon which are dominated by coastal upwelling. This mid-latitude site is easily accessible by small boat from the Oregon State University marine facility at Newport, Oregon. We plan to collect regular monthly samples of bio-optical and standard biological variables during the first years of AM-1.

The basic in situ observations for ocean color studies are well-documented in the SIMBIOS plan and the relevant SeaWiFS technical memoranda. The only extension that will be needed for FLH is to ensure that radiance measurements are made at the appropriate wavelengths (nominally 667, 678, and 748 nm).

Primary productivity measurements are also part of the standard SeaWiFS/SIMBIOS suite. We will also include FRR fluorometry as part of the field measurement set.

The simplest measures of success will be the ability of the algorithms to perform within predicted error limits over a broad range of environmental conditions. For example, after the initial validation stage, can the algorithms be applied in different ocean regions or different atmospheric conditions and continue to produce data sets within the expected error? The second measure will be an assessment of the stability of the data products over a long time period. For example, are there unexplained biases in the long-term record or unexpected seasonal trends? The third measure is the most stringent and is based on the performance of numerical models that assimilate these data products. In this case, tests will be based on the adequacy of the estimates of error fields as well as an evaluation of model performance. For example, have we sufficiently quantified the temporal and spatial error fields of the data products so that assimilation techniques can be applied? Do numerical models perform better if the data sets are assimilated into the model?

<u>3.2.3 Quality Control and Diagnostics</u>

In regards to quality control, much of it will done as part of the routine processing at the DAAC. A set of seven flags will be evaluated for each pixel. The first flag will be a 2-bit summary flag that will quantify the flags produced by the input products (MOD 18 and MOD19). The summary flag will depend on the severity of the input flag. For example, a failure of the atmospheric correction algorithm will cause the summary flag to be set to 11. The presence of coccoliths will set the summary flag to 01.

Six flags will be set to indicate quality of the FLH product. These flags are listed in Table 2. The first two flags will warn users that the FLH value is outside the expected range. The third and fourth flags indicate atypical conditions for the FLH algorithm. For example, the radiance in band 15 will be higher than the radiance in band 13. Although the FLH peak in band 14 is usually higher than the baseline, this is not an absolute requirement. The number of pixels used to calculate FLH can also vary, and this will be indicated in the fifth flag. Finally, in areas of high noise (or few valid pixels), the coefficient of variation may be high.

Flag Number	Condition
FLH_1	FLH below expected range
FLH_2	FLH above expected range
FLH_3	Wrong baseline slope (band 15 > band 13)
FLH_4	FLH below baseline
FLH_5	Number of pixels used to calculate FLH
00	1 pixel used
01	2-8 pixels used
10	9-15 pixels used
11	16 or more pixels used
FLH_6	High coefficient of variation

Table 2. Quality flags for FLH

Another set of flags will be produced to guide time/space binning of FLH. Our initial approach is to include only those pixels corresponding to the "best" ranking within the time/space bin. A simple arithmetic average will be calculated of these "best" pixels. For example, if there are only three pixels of Rank #1 in the bin, then average only these three pixels. If there are no Rank #1 pixels, then average only pixels of Rank # 2 and so on.

15

The CFE quality flags are similar to the FLH flags, except that some of them will depend on the MOD22 (ARP) flags.

3.2.4 Exception Handling

Much of the exception handling will be performed in the Miami system; cloud detection line dropouts, etc. will be done before the radiances are delivered to the FLH algorithm. These tests are discussed in the appropriate ATBD.

3.2.5 Data Dependencies

The only dependencies for the FLH calculation are those necessary to calculate the basic normalized water-leaving radiances. The Case 1 chlorophyll (MOD19) is used to determine whether FLH should be calculated at the full resolution of MODIS or if it should be based on a 5 by 5 bin. There are no other inputs required for the FLH calculation. CFE will depend on ARP.

It should be noted that eventually we will wish to produce a comprehensive FLH product using all of the available sensors. Thus we will need access to MERIS and GLI data sets as well as data from both MODIS sensors.

3.2.6 Output Product

The FLH and CFE products will consist of the data value plus a set of flags described above. A data value will be present at each pixel.

4.0 Constraints, Limitations, Assumptions

FLH depends on the production of calibrated radiances at three wavelengths: 667, 678, and 748 nm. These values will be produced in the MODIS Oceans Team processing stream being developed at the University of Miami. Assumptions associated with this part of the processing can be found in the appropriate ATBD.

The most critical assumption is that atmospheric effects can be removed with a simple model from the three wavelengths used to calculate FLH. This assumption is based on the following observations. The dominant atmospheric effect in the visible wavelengths is molecular or Rayleigh scattering. As this type of scattering varies as $1/\lambda^4$, then its effect is fairly small at the wavelengths of interest to the FLH calculation. At longer wavelengths, the primary impact of the atmosphere is in the form of absorption, rather than scattering. In particular, oxygen absorption bands at 687 and 762 nm and water vapor bands at 656 and 730 nm are potentially troublesome. MODIS was designed specifically to minimize the impact of these absorption features on the FLH calculation.

Petterrson et al. (1990) presents data showing the changes in spectra with altitude. In general, the amount of correction is small in the longer wavelengths (greater than about 650 nm) except near absorption features. Although the MODIS design should minimize atmospheric effects, it is clear that several tests must be performed on actual MODIS data to ensure that the estimates of FLH do not vary strongly with changes in atmospheric conditions or path length. If correction is needed, then we will work with Howard Gordon to develop a correction scheme, probably based on that used for shorter wavelengths. This should be relatively straightforward, as the bands that will need correction are close to the 865 nm band that will be used for correcting the other ocean data products.

This approach assumes that backscattered sunlight will not pose a significant problem. This may not be the case in waters with heavy particulate loads where backscattering near the ocean surface may be intense. Because particulate materials such as detritus scatter light in the red wavelengths, some of the FLH signal may simply be backscattered sunlight rather than chlorophyll fluorescence. Most in situ measurements are made well below the penetration depth of sunlight at 683 nm so that the measured signal arises from fluorescence. This constraint does not affect the FLH algorithm but it will influence the interpretation of the data. Roesler and Perry (1995) suggests a method that defines the fluorescence term separately from the backscatter components. This approach relies on the angular distribution of incoming

irradiance and the separation of absorption and backscattering. However, given the limited spectral information present in MODIS, it appears that the simple baseline may be adequate.

Both CFE and FLH will be calculated only for non-cloud, glint-free ocean pixels during daylight hours. Such conditions will be based on tests incorporated into the Miami processing system.

The use of FLH and CFE as indicators of phytoplankton photosynthetic state will require considerably more research. FLH has been used successfully as a measure of chlorophyll concentration, especially in Case 2 waters (Petterrson et al. 1990). Although there are several papers on the use of sun-stimulated fluorescence to estimate primary productivity, no one has attempted the use of FLH to estimate productivity from aircraft. MODIS represents the first attempt to measure fluorescence from space, and as such, will require considerable research. Many investigators are studying the relationship between fluorescence and productivity, and our research will build on these results.

References

Abbott, M.R., P.J. Richerson, and T.M. Powell, In situ response of phytoplankton fluorescence to rapid variations in light, Limnol. Oceanogr., 27, 218-225, 1982.

Abbott, M.R., K.H. Brink, C.R. Booth, D. Blasco, M.S. Swenson, C.O. Davis, and L.A. Codispoti, Scales of variability of bio-optical processes as observed from near-surface drifters, J. Geophys. Res., 100, 13,345-13,367.

Austin, R.W., Gulf of Mexico, ocean-colour surface-truth measurements, Boundary-layer Meteorol., 18, 269-285, 1980.

Borstad, G.A., H.R. Edel, J.F.R. Gower, and A.B. Hollinger, Analysis of test and flight data from the Fluorescence Line Imager, Canadian Spec. Pub Fish. Aquat. Sci. 83, 1985.

Butler, W.L., Energy distribution in the photochemical apparatus of photosynthesis, Ann. Rev. Plant Physiol., 29, 345-378, 1978.

Chamberlin, W.S., and J. Marra, Estimation of photosynthetic rate from measurements of natural fluorescence: Analysis of the effects of light and temperature, Deep Sea Res., 39, 1695-1706, 1992.

Chamberlin, W.S., C.R. Booth, D.A. Kiefer, J.H. Morrow, and R.C. Murphy, Evidence for a simple relationship between natural fluorescence, photosynthesis, and chlorophyll in the sea, Deep Sea Res., 37, 951-973, 1990.

Clark, D.K., Phytoplankton pigment algorithms for the Nimbus-7 CZCS, in Oceanography from Space, edited by J.F.R. Gower, pp. 227-238, Plenum Press, New York, 1981.

Falkowski, P., and D.A. Kiefer, Chlorophyll *a* fluorescence in phytoplankton: Relationship to photosynthesis and biomass, J. Plankton Res., 7, 715-731, 1985.

Falkowski, P.G., and Z. Kolber, Estimation of phytoplankton photosynthesis by active fluorescence, ICES Mar. Sci. Symp., 197, 92-103, 1993.

Falkowski, P., and Z. Kolber, Variations in quantum yield of photosynthesis in marine phytoplankton as measured by active fluorescence, EOS Trans. Amer. Geophys. Union (abstract), 75, 232, 1994.

Fischer, J., and U. Kronfeld, Sun-stimulated chlorophyll fluorescence, 1: Influence of oceanic properties, Int. J. Remote Sensing, 11, 2125-2147, 1990.

Fischer, J., and P. Schlüssel, Sun-stimulated chlorophyll fluorescence, 2: Impact of atmospheric properties, Int. J. Remote Sensing, 11, 2149-2162, 1990.

Frouin, R.J., M. Schwindling, and P.-Y. Deschamps, Spectral reflectance of sea foam in the visible and near-infrared: In situ measurements and remote sensing implications, J. Geophys. Res., 101, 14,361-14,371, 1996.

Gordon, H.R., Diffuse reflectance of the ocean: The theory of its augmentation by chlorophyll *a* fluorescence at 685 nm, Appl. Optics, 18, 1161-1166, 1979.

Gower, J.F.R., Observations of in situ fluorescence of chlorophyll *a* in Saanich Inlet, Boundary Layer Met., 18, 235-245, 1980.

Gower, J.F.R., and G.A. Borstad, Use of in vivo fluorescence line at 685 nm for remote sensing surveys of surface chlorophyll *a*, in Oceanography from Space, edited by J.F.R. Gower, pp. 329-338, Plenum, New York, 1981.

Gower, J.F.R., and G.A. Borstad, On the use of solar-stimulated fluorescence signal from chlorophyll *a* for airborne and satellite mapping of phytoplankton, Adv. Space Res., 7, 101-106, 1987.

Gower, J.F.R., and G.A. Borstad, Mapping of phytoplankton by solar-stimulated fluorescence using an imaging spectrometer, Int. J. Remote Sensing, 11, 313-320, 1990.

Holm-Hansen, O., C.J. Lorenzen, R.W. Holmes, and J.D.H. Strickland, Fluorometric determination of chlorophyll, J. Cons. Cons. Int. Explor. Mer, 30, 3-15, 1965.

Kiefer, D.A., Fluorescence properties of natural phytoplankton populations, Mar. Biol., 22, 263-269, 1973*a*.

Kiefer, D.A., Chlorophyll *a* fluorescence in marine centric diatoms: Response of chloroplasts to light and nutrients, Mar. Biol, 23, 39-45, 1973*b*.

Kiefer, D.A., W.S. Chamberlin, and C.R. Booth, Natural fluorescence of chlorophyll *a*: Relationship to photosynthesis and chlorophyll concentration in the western South Pacific gyre, Limnol. Oceanogr., 34, 868-881, 1989.

Kiefer, D.A., and R.A. Reynolds, Advances in understanding phytoplankton fluorescence and photosynthesis, in Primary Productivity and Biogeochemical Cycles in the Sea, edited by P.G. Falkowski and A.D. Woodhead, pp. 155-174, Plenum, New York, 1992.

Kirk, J.T.O., Light and Photosynthesis in Aquatic Ecosystems. 2d Ed, Cambridge University Press, New York, 509 pp., 1994.

Kishino, M., S. Sugihara, and N. Okami, Influence of fluorescence of chlorophyll *a* on underwater upward irradiance spectrum, La Mer, 22, 224-232, 1984.

Kneizys, F.X., Shettle, E.P., Abreu, L.W., Chetwynd, J.H., Anderson, G.P., Gallery, W.O. , Selby, J.E.A., Clough, S.A., Users Guide to LOWTRAN 7. Air Force Geophysics Laboratory report # AFGL-TR-88-0177, 137 pp., 1988.

Kolber, Z., and Falkowski, P.G., Use of active fluorescence to estimate phytoplankton photosynthesis in situ, Limnol. Oceanogr., 38, 1646-1665, 1993.

Krause, G.H., and E. Weis, Chlorophyll fluorescence and photosynthesis: The basics, Ann. Rev. Plant Physiol. Plant Mol. Biol., 42, 313-349, 1991.

Letelier, R.M., and M.R. Abbott, An analysis of chlorophyll fluorescence algorithms for the Moderate Resolution Imaging Spectrometer (MODIS), Rem. Sensing Environ., in press, 1996.

Letelier, R.M., M.R. Abbott, and D.M. Karl, Chlorophyll natural fluorescence response to upwelling-induced iron pulses in the Southern Ocean, Geophys. Res. Letters, submitted, 1996.

Lorenzen, C.J., A method for the continuous measurement of in vivo chlorophyll concentration, Deep Sea Res., 13, 223-227, 1966.

Neville, R.A., and J.F.R. Gower, Passive remote sensing of phytoplankton via chlorophyll *a* fluorescence, J. Geophys. Res., 82, 3487-3493, 1977.

Petterrson, L.H., Ø. Frette, O. Johannessen, K. Sørensen, G. Borstad, R. Kerr, and J.F.R. Gower, NORSMAP '89, Nansen Remote Sensing Centre, Tech. Rep. 28, 1990.

Prézelin, B.B., Light reactions in photosynthesis, in Physiological Bases of Phytoplankton Ecology, edited by T. Platt, pp. 1-43, Can. Bull. Fish. Aquat. Sci., 210, 1981.

Roesler, C.S., and M.J. Perry, In situ phytoplankton absorption, fluorescence emissions, and particulate backscattering spectra determined from reflectance, J. Geophys. Res., 100, 13,279-13,294, 1995.

Samuelsson, G., and G. Öquist, A method for studying photosynthetic capacities of unicellular algae based on in vivo chlorophyll fluorescence, Physiol. Plant, 40, 315-319, 1977.

Smith, R.C., and K.S. Baker, Optical classification of natural waters, Limnol. Oceanogr., 23, 260-267., 1978.

Smith, R.C., and K.S. Baker, Optical properties of the clearest natural waters (200-800 nm), Appl. Opt., 20, 177-193, 1981.

Stegmann, P.M., M.R. Lewis, C.O. Davis, and J.J. Cullen, Primary production estimates from recordings of solar-stimulated fluorescence in the equatorial Pacific at 150° W, J. Geophys. Res., 97, 627-638, 1992.

Topliss, B.J., Optical measurements in the Sargasso Sea: Solar-stimulated chlorophyll fluorescence, Oceanol. Acta, 8, 263-270, 1985.

Topliss, B.J., and T. Platt, Passive fluorescence and photosynthesis in the ocean: Implications for remote sensing, Deep Sea Res., 33, 849-864, 1986.